

## Supporting Information

# **A 16.4% Efficiency Organic Photovoltaic Cell Enabled Using Two Donor Polymers with Their Side-Chains Oriented Differently by a Ternary Strategy**

Yuan Chang<sup>a,b,c</sup>, Tsz-Ki Lau<sup>d</sup>, Philip CY Chow<sup>c</sup>, Ningning Wu<sup>b</sup>, Dan Su<sup>b</sup>,  
Weichao Zhang<sup>a,b</sup>, Huifeng Meng<sup>b</sup>, Chao Ma<sup>e</sup>, Tao Liu<sup>c</sup>, Kun Li<sup>b</sup>, Kam  
Sing Wong<sup>e</sup>, Xinhui Lu<sup>d</sup>, He Yan<sup>c\*</sup> and Chuanlang Zhan<sup>a,b\*</sup>

<sup>a</sup> College of Chemistry and Environmental Science, Inner Mongolia Normal University,  
Huhhot 010022, China.

<sup>b</sup> Beijing National Laboratory for Molecular Sciences, CAS key Laboratory of  
Photochemistry, Institute of Chemistry, Chinese Academy of Sciences, Beijing 100190, China.

<sup>c</sup> Department of Chemistry, The Hong Kong University of Science and Technology, Clear  
Water Bay, Kowloon, Hong Kong, China.

<sup>d</sup> Department of Physics, Chinese University of Hong Kong, New Territories, Hong  
Kong, China.

<sup>e</sup> Department of Physics, Hong Kong University of Science and Technology, Clear Water Bay,  
Kowloon, Hong Kong, China

\* E-mail: clzhan@iccas.ac.cn (C.Z.), hyan@ust.hk (H.Y.)

## Materials, methods, and characterizations

**Materials.** The materials of PBDB-T-SF, PBDB-T-2F, Y6, PEDOT:PSS and PDINO were purchased from Solarmer company.

**UV-Vis absorption spectra.** Absorption spectra of donor polymers and acceptors in solid thin films were prepared by spin-coating their solutions atop the quartz glass substrates and measured on a Hitachi U-3010 UV–vis spectrophotometer.

**Cyclic voltammetry measurements.** For CV experiments, the compound was fully dissolved in N<sub>2</sub>-degassed anhydrous CHCl<sub>3</sub> with a concentration of 10<sup>-4</sup> M and then the solution was deposited onto the work electrode surface to form a thin solid film. CV traces were measured on an electrochemical workstation (CHI 660) at a scan rate of 50 mV/s using tetrabutylammonium tetrafluoroborate (Bu<sub>4</sub>NBF<sub>4</sub>) as the supporting electrolyte. A glassy carbon electrode, a Pt wire and an Ag/AgCl electrode were used as the working, counter and reference electrodes, respectively.

**AFM characterizations.** The AFM images were recorded using a Bruker multimode 8 AFM.

**TFM characterizations.** TEM experiments were performed on a JEM-2100 transmission electron microscope operated at 200 kV. For TEM experiments, the films were obtained by transferring the floated blend films from the water onto the Cu grid.

**Solar cell fabrications and characterizations.** Devices were fabricated on the Indium tin oxide (ITO) patterned glass with a conventional configuration of ITO/PEDOT:PSS/active layers/PDINO/Al. The ITO substrates with a sheet resistance of 10 ohm/square and transmission rate of 90% were firstly cleaned by detergent, deionized water, acetone and isopropanol in turn with sonication for 30 min respectively. The substrates were dried by nitrogen gas and then treated by UV-Ozone for 30 min before use. PEDOT:PSS was spin-coated onto the ITO substrates at 6000 rpm for 30 s, then the substrates were moved to oven and dried at 150°C for 15 min. The PBDB-T-SF: PBDB-T-2F: Y6 blends with different weight ratio were dissolved in chloroform (CF) (the total concentration of the solution was 16 mg/mL). The blend solution was spin-coated on the top of PEDOT:PSS layer followed by solvent vapor annealing (CF), and then thermal annealing was utilized to optimize the morphology of active layer. The optimal method for active layer was to deposit the solution with 0.60% CN at 3000 rpm and annealed at 90°C for 10 minutes. Atop the active layer, a thin electron transporting layer of PDINO (1.0 mg/mL in methanol, 3000 rpm for 30 s, about 15 nm) was spin-coated. Finally, the Al electrodes were thermally deposited on the top of devices, the thickness of which was about 100 nm.

The current density – voltage ( $J - V$ ) curves were measured in a nitrogen glove box and were conducted on a computer-controlled Keithley 2400 source measure unit under AM 1.5G (calibrated to be 100 mW/cm<sup>2</sup> with a reference silicon cell) using a solar illumination (AAA grade, XES-70S1). The series and shunt resistances were obtained directly from the illuminated  $J - V$  curves of the

optimal devices, which are given out along with the solar cell parameters such as  $V_{oc}$ ,  $J_{sc}$ , FF and PCE directly by the measurement software provided by Enli Technology Co. Ltd, Taiwan. The EQE measurements were performed with the as-fabricated solar cell using a QE-R3011 instrument (Enli Technology Co. Ltd., Taiwan).

**SCLC measurements.** The electron and hole mobilities were measured by using the method called space-charge limited current (SCLC) for electron-only and hole-only devices. The structure of electron-only devices was ITO/titanium (diisopropoxide) bis(2,4-pentanedionate) (TIPD)<sup>[11]</sup>/active layer/PDINO/Al and the hole-only devices were fabricated with the structure of ITO/PEDOT:PSS/active layer/Au. The charge carrier mobility was determined by fitting the dark current to the model of a single carrier SCLC according to the Mott–Gurney law:  $J = 9\varepsilon_0\varepsilon_r\mu V^2/8L^3$ , where  $J$  is the measured current density,  $L$  is the film thickness of the active layer,  $\mu$  is the mobility of charge carrier,  $\varepsilon_r$  is the relative dielectric constant of the transport medium component, here a value of 3.0 was used for calculations of the mobilities, and  $\varepsilon_0$  is the permittivity of vacuum ( $8.85419 \times 10^{-12} \text{ CV}^{-1}\text{m}^{-1}$ ),  $V$  is the difference of applied voltage ( $V_{app}$ ) and offset voltage ( $V_{BI}$ ). The mobility of charge carriers can be calculated from the slope of the  $J^{1/2} \sim V$  curves.

**GIWAXS measurements.** GIWAXS data was carried out with a Xeuss 2.0 SAXS/WAXS laboratory beamline using a Cu X-ray source (8.05 keV, 1.54 Å) and Pilatus3R 300K detector. The incidence angle is 0.2°.

**DFT calculations.** The calculations were performed on a Gauss software package on 6-31G\*\* level.

#### **Transient photocurrent (TPC) and transient photovoltage (TPV)**

The measurements were performed with device under steady-state illumination from a focused Quartz Tungsten-Halogen Lamp light source which raised background response similar to open-circuit voltage. An optical perturbation is applied to the device with a 1 kHz femtosecond pulse laser under 550 nm excitation. The TPC signal was acquired by a digital oscilloscope at open-circuit condition. The TPC signal was acquired under approximately short-circuit condition by applying a 100 Ω resistor. The fitting function of  $y=y_0+A_1*\exp(-x/t_1)$  was used. Parameters obtained from the fitting curve were displayed in the following table. In the table,  $t_1$  is carrier lifetime,  $k$  is kinetic reaction rate constant and  $\tau$  is  $t_1*\ln 2$ . Adj.  $R^2$  describing the fitting quality is also included.

#### **Solid-state <sup>19</sup>F MAS NMR (magic angle spinning nuclear magnetic microscopy)**

The solid-state <sup>19</sup>F MAS NMR spectra were recored on a Bruker AVANCE III 400 solid-state NMR Spectrometer with 2.5mm H-F-X Probe. The spinning speed is 20kHz. A recycle delay time of 1s is selected. <sup>19</sup>F chemical shift is referenced to KF at -133.40 ppm.

## Supporting figures

**Figure S1.** Traces of cyclic voltammetry (CV) of PBDB-T-SF (a), PBDB-TF (b), and Y6 (c) with ferrocene used as a reference.

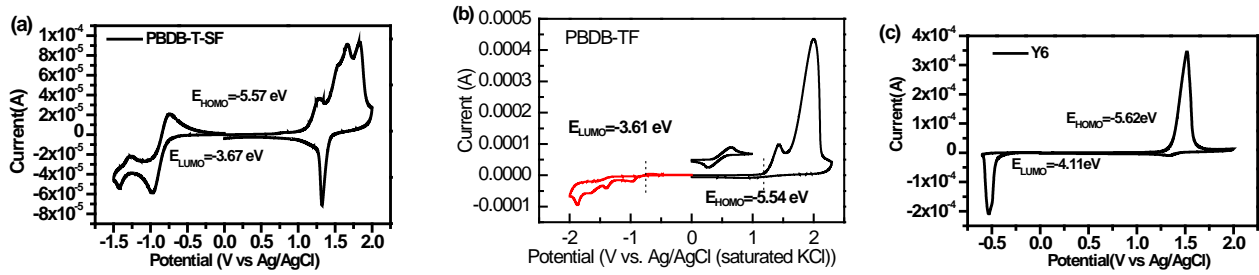


**Figure S2.** Scanning copy of the certificate report of the optimal device with PBDB-TF:PBDB-T-SF:Y6 (0.85:0.15:1.2) as the active layer and PDINO as the ETL obtained from the National Institute of Metrology (NIM), China.

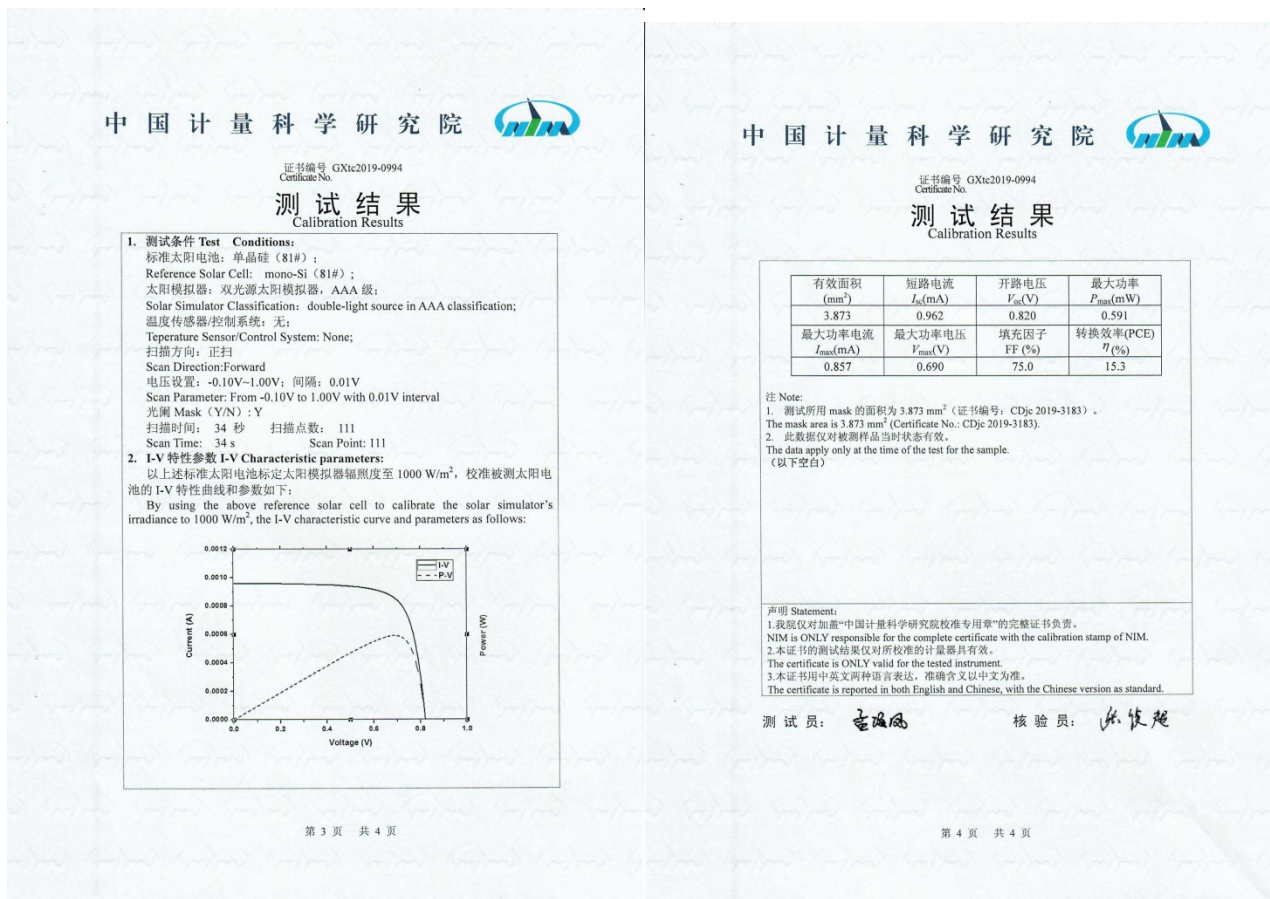


**Figure S3.** The dark  $J - V$  curves of the optimal binary and ternary solar cells.

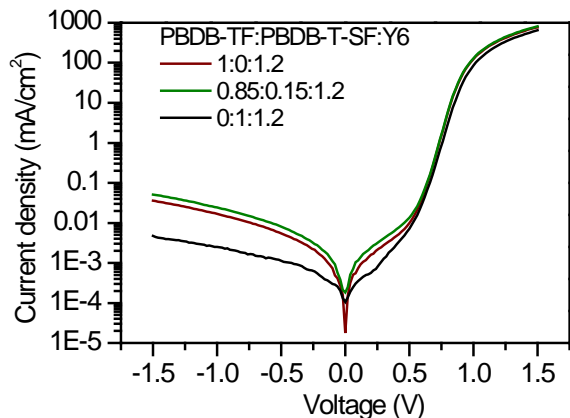


**Figure S4.** The  $J^{0.5} - V$  plots for calculations of the electron (a) and hole (b) mobilities of the binary and ternary blends.

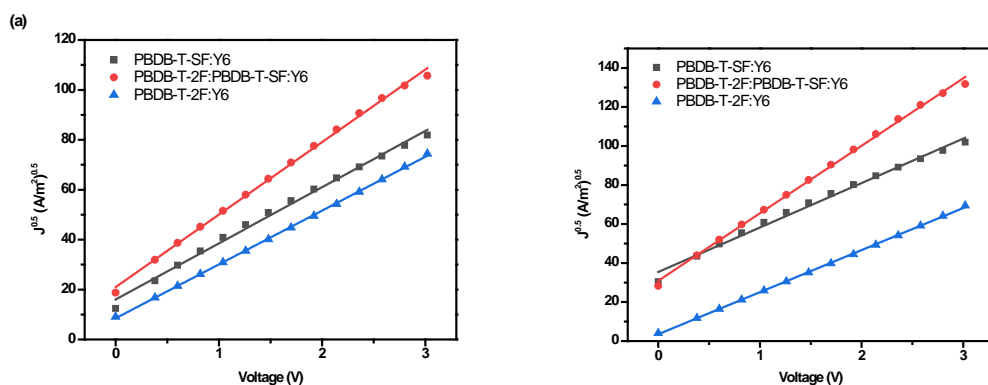


**Figure S5.** 2-D GIWAXS images (a-c) of the binary and ternary blended films, respectively.

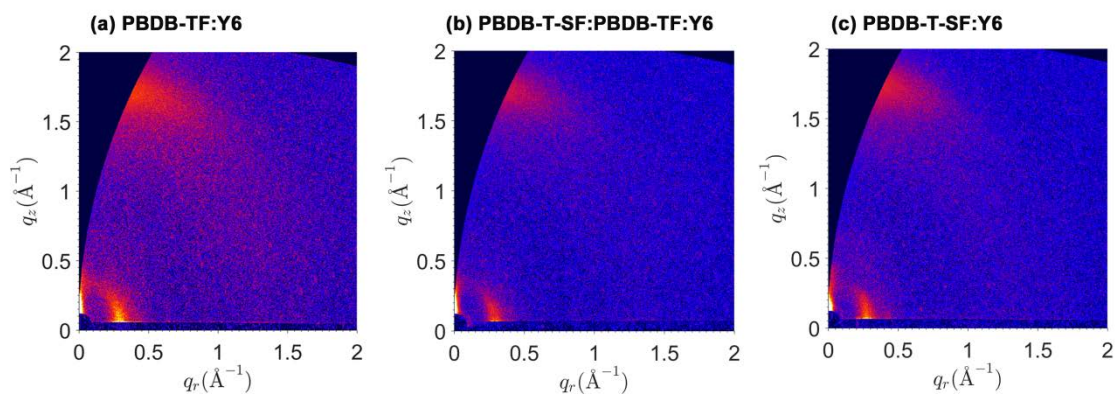
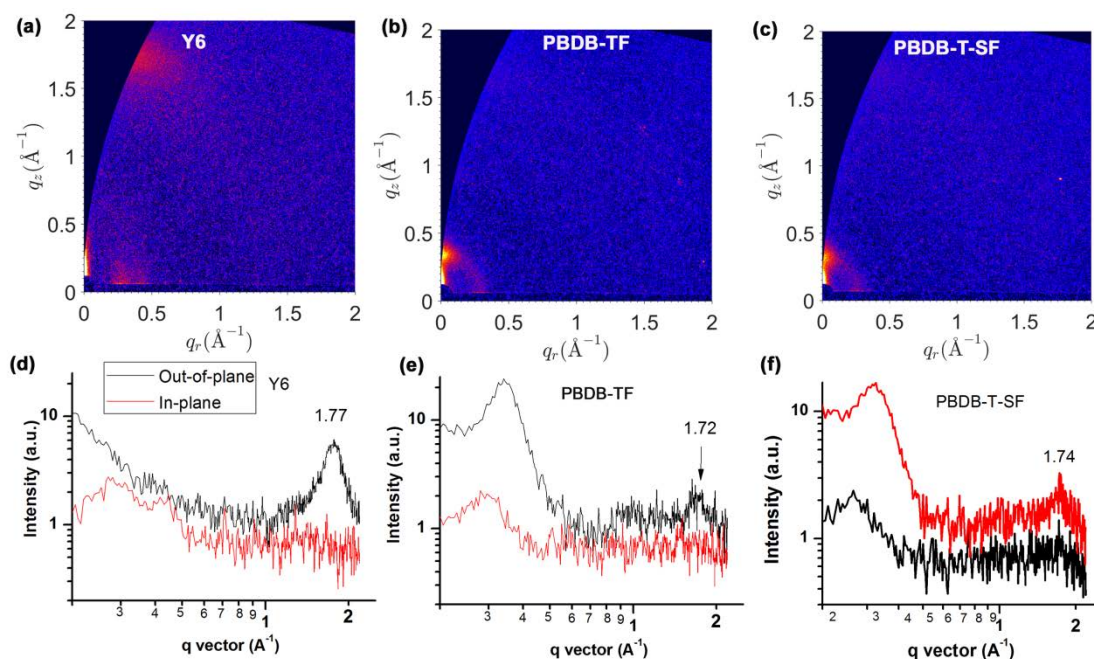


**Figure S6.** Two-dimensional pictures of the GIWAXS data (a-c) and the linecut profiles (d-f) of the pure Y6 (a and d), PBDB-TF (b and e) and PBDB-T-SF (c and f) films.



## Supporting Tables

**Table S1.** The photovoltaic data of ternary solar cells with different optimized conditions.

Conditions		$V_{oc}^a$ [V]	$J_{sc}^a$ [mA/cm <sup>2</sup> ]	$FF^a$ [%]	$PCE_{ave}^a$ [%]
PBDB-TF: PBDB-T-SF	100:0	0.848 (0.842±0.004)	24.83 (24.17±0.48)	73.60 (71.35±1.37)	15.50 (15.03±0.42)
	95:5	0.852 (0.845±0.005)	24.97 (24.43±0.50)	74.72 (72.59±1.42)	15.91 (15.36±0.56)
	85:15	0.856 (0.850±0.004)	25.21 (24.53±0.42)	76.11 (74.36±1.63)	16.42 (15.89±0.47)
	75:25	0.857 (0.852±0.003)	24.84 (24.25±0.35)	73.24 (71.12±1.58)	15.59 (14.87±0.51)
	60:40	0.858 (0.852±0.005)	24.33 (23.85±0.52)	72.66 (70.98±1.67)	15.17 (14.52±0.49)
	0:100	0.862 (0.853±0.004)	24.68 (24.07±0.38)	71.19 (69.65±1.36)	15.15 (14.74±0.38)
CN (%)	0.2	0.861 (0.855±0.003)	24.35 (23.74±0.51)	73.64 (71.98±1.41)	15.44 (14.87±0.38)
	0.4	0.858 (0.851±0.005)	24.61 (24.11±0.48)	74.76 (72.58±1.59)	15.76 (15.83±0.51)
	0.6	0.856 (0.850±0.004)	25.21 (24.53±0.42)	76.11 (74.36±1.63)	16.42 (15.89±0.47)
	0.8	0.850 (0.845±0.003)	24.46 (24.01±0.35)	72.47 (72.19±1.84)	15.06 (15.58±0.46)
Annealing temperature (°C)	80	0.860 (0.853±0.003)	24.73 (23.95±0.39)	74.92 (73.15±1.49)	15.95 (15.24±0.42)
	90	0.856 (0.850±0.004)	25.21 (24.53±0.42)	76.11 (74.36±1.63)	16.42 (15.89±0.47)
	100	0.851 (0.846±0.004)	24.94 (23.78±0.45)	75.59 (73.67±1.74)	16.04 (15.41±0.53)

**Table S2.** The parameters obtained by fitting the experimental TPC and TPV data with Eq  $y=y_0+A_1*\exp(-x/t_1)$ , here,  $t_1$  is carrier lifetime,  $k$  is kinetic reaction rate constant,  $\tau$  is  $t_1*\ln 2$ . Adj.  $R^2$  describes the fitting quality.

Devices	$y_0$	$A_1$	$t_1$ [s]	$K_{rec}$ [s <sup>-1</sup> ]	$\tau$ [s]	Adj. $R^2$	
TPC	PBDB-TF binary	-0.00690	0.94103	5.02E-07	1.99E+06	3.48E-07	0.9923
	Ternary	-0.00722	0.89901	4.26E-07	2.35E+06	2.96E-07	0.9821
	PBDB-T-SF binary	-0.00239	1.09334	4.91E-07	2.04E+06	3.40E-07	0.9977
TPV	PBDB-TF binary	0.01050	0.98728	1.52E-07	6.59E+06	1.05E-07	0.9923
	Ternary	0.01367	1.00627	1.89E-07	5.29E+06	1.31E-07	0.9951
	PBDB-T-SF binary	-0.00527	1.12390	1.14E-07	8.79E+06	7.89E-08	0.9978

## References

- [1] Z. Tan, W. Zhang, Z. Zhang, D. Qian, Y. Huang, J. Hou, Y. Li, *Advanced Materials* 2012, 24, 1476.